Subdiffraction incoherent optical imaging via spatial-mode demultiplexing: semiclassical treatment

Mankei Tsang[1,2,*]

[1]*Department of Electrical and Computer Engineering, National University of Singapore, 4 Engineering Drive 3, Singapore 117583*
[2]*Department of Physics, National University of Singapore, 2 Science Drive 3, Singapore 117551*

(Dated: March 28, 2017)

I present a semiclassical analysis of a recently proposed spatial-mode demultiplexing (SPADE) measurement scheme for the far-field imaging of spatially incoherent optical sources [M. Tsang, New J. Phys. **19**, 023054 (2017)]. Using only basic concepts in statistical optics, I derive the errors of estimating the object moments with SPADE and simple linear estimators, proving that they can be much lower than the errors with direct imaging for subdiffraction objects.

arXiv:1703.08833v1 [physics.optics] 26 Mar 2017

I. INTRODUCTION

Recent breakthroughs suggest that far-field measurement methods can substantially improve the imaging of subdiffraction incoherent sources [1–16]. In particular, Ref. [16] shows that a spatial-mode demultiplexing (SPADE) scheme can estimate the second and higher moments of an arbitrary source distribution much more precisely than direct imaging can fundamentally do in the subdiffraction regime. While the predicted enhancements are promising for applications in both fluorescence microscopy and astronomy, the theory relies on a quantum formalism that may be difficult to comprehend for researchers in those fields. Here I introduce a semiclassical treatment that reproduces most of the results, assuming only knowledge of the mutual coherence function and Poisson statistics on the level of Goodman's textbooks [17, 18]. I also derive more rigorous expressions for the achievable errors without an approximation used in Ref. [16], demonstrating more convincingly the superiority of SPADE over direct imaging.

II. STATISTICAL OPTICS

Consider the paraxial theory of quasi-monochromatic scalar waves and a spatially incoherent source distribution [17, 18]. On the image plane of a diffraction-limited imaging system, the mutual coherence function, also called the mutual intensity, can be expressed as [17, 18]

$$\Gamma(\boldsymbol{r},\boldsymbol{r}'|\theta) = N\int d^2\boldsymbol{R}\psi(\boldsymbol{r}-\boldsymbol{R})\psi(\boldsymbol{r}'-\boldsymbol{R})F(\boldsymbol{R}|\theta), \quad (2.1)$$

where $F(\boldsymbol{R}|\theta)$ is the object intensity distribution, $\boldsymbol{R} = (X,Y)$ is the two-dimensional object-plane position vector, θ is a vector of unknown parameters to be estimated, $\psi(\boldsymbol{r})$ is the field point-spread function (PSF), and $\boldsymbol{r} = (x,y)$ and $\boldsymbol{r}'$ are image-plane position vectors. For convenience, the image-plane coordinates are normalized with respect to the magnification factor, and all the position coordinates are also normalized with respect to the PSF width, such that they are dimensionless and the PSF width is 1 in this dimensionless unit. The other assumed normalization conditions are

$$\int d^2\boldsymbol{r}|\psi(\boldsymbol{r})|^2 = 1, \qquad \int d^2\boldsymbol{R}F(\boldsymbol{R}|\theta) = 1, \quad (2.2)$$

and

$$N = \int d^2\boldsymbol{r}\Gamma(\boldsymbol{r},\boldsymbol{r}|\theta), \quad (2.3)$$

which is taken to be the total expected energy over a given observation time. The expected intensity distribution on the image plane becomes

$$\Gamma(\boldsymbol{r},\boldsymbol{r}|\theta) = N\int d^2\boldsymbol{R}|\psi(\boldsymbol{r}-\boldsymbol{R})|^2F(\boldsymbol{R}|\theta), \quad (2.4)$$

which is a basic result in statistical optics.

Instead of measuring the intensity, if the image-plane field is processed further via passive and lossless linear optics, the expected energy in each output channel can be expressed as

$$\bar{m}_j(\theta) = \int d^2\boldsymbol{r}\int d^2\boldsymbol{r}'\phi_j^*(\boldsymbol{r})\phi_j(\boldsymbol{r}')\Gamma(\boldsymbol{r},\boldsymbol{r}'|\theta) \quad (2.5)$$

$$= N\int d^2\boldsymbol{R}\left|\int d^2\boldsymbol{r}\phi_j^*(\boldsymbol{r})\psi(\boldsymbol{r}-\boldsymbol{R})\right|^2 F(\boldsymbol{R}|\theta). \quad (2.6)$$

Energy conservation implies that the projection into mode functions $\phi_j^*(\boldsymbol{r})$ is a unitary operation, satisfying

$$\int d^2\boldsymbol{r}\phi_j(\boldsymbol{r})\phi_k^*(\boldsymbol{r}) = \delta_{jk}. \quad (2.7)$$

In other words, $\{\phi_j(\boldsymbol{r})\}$ is an orthonormal basis, and any linear optics can be regarded as mode demultiplexing [3, 19]. For example, direct imaging, which measures the spatial intensity distribution on the image plane, can be modeled with $\phi_j(\boldsymbol{r}) = \sqrt{d^2\boldsymbol{r}}\delta^2(\boldsymbol{r}_j-\boldsymbol{r})$, where $\boldsymbol{r}_j$ is the position of each pixel with infinitesimal area $d^2\boldsymbol{r}$, such that $\bar{m}_j(\theta) = d^2\boldsymbol{r}\Gamma(\boldsymbol{r}_j,\boldsymbol{r}_j|\theta)$. Optical losses can be modeled by introducing ancillary inaccessible channels to the lossless model [3].

For weak incoherent sources, such as astronomical thermal sources and microscopic fluorophores at optical frequencies, bunching or antibunching is negligible, and it is standard to assume a Poisson model for the photon counts $m =$

* mankei@nus.edu.sg

$(m_1, m_2, \dots)$ at the output channels [3, 18, 20–23]. If $\bar{m}_j(\theta)$ is normalized in the unit of photon number, the probability distribution is

$$P(m|\theta) = \prod_j e^{-\bar{m}_j(\theta)} \frac{[\bar{m}_j(\theta)]^{m_j}}{m_j!}. \tag{2.8}$$

The quantum formalism arrives at the same conclusion by assuming the average photon number per mode to be much smaller than 1 and integrating the photon count of each channel over multiple temporal modes [1, 16]. The most important statistics here are the mean

$$\mathbb{E}(m_j) = \bar{m}_j(\theta), \tag{2.9}$$

and the covariance matrix

$$\mathbb{E}(m_j m_k) - \mathbb{E}(m_j)\mathbb{E}(m_k) = \bar{m}_j(\theta)\delta_{jk}, \tag{2.10}$$

where the expectation is defined as

$$\mathbb{E}(f) \equiv \sum_m f(m) P(m|\theta). \tag{2.11}$$

Let the parameters of interest be the object moments defined as

$$\theta_{\boldsymbol{\mu}} = \int d^2\boldsymbol{R} \boldsymbol{R}^{\boldsymbol{\mu}} F(\boldsymbol{R}|\theta), \quad \boldsymbol{\mu} = (\mu_X, \mu_Y) \in \mathbb{N}^2, \tag{2.12}$$

$$\boldsymbol{R}^{\boldsymbol{\mu}} \equiv X^{\mu_X} Y^{\mu_Y}, \qquad \mathbb{N} \equiv \{0, 1, 2, \dots\}. \tag{2.13}$$

Define the object width as the minimum Δ such that

$$F(\boldsymbol{R}|\theta) = 0 \text{ for } |\boldsymbol{R}| > \frac{\Delta}{2}, \tag{2.14}$$

and define the scenario where Δ is much smaller than the PSF width, or

$$\Delta \ll 1, \tag{2.15}$$

as the subdiffraction regime. Assuming the Gaussian PSF

$$\psi(\boldsymbol{r}) = \frac{1}{\sqrt{2\pi}} e^{-|\boldsymbol{r}|^2/4}, \tag{2.16}$$

which is a common assumption in fluorescence microscopy [22, 23], Ref. [16] shows that the Cramér-Rao bound (CRB) [20, 22–24] for direct imaging is

$$\mathbb{E}\left(\check{\theta}_{\boldsymbol{\mu}} - \theta_{\boldsymbol{\mu}}\right)^2 \geq \frac{\boldsymbol{\mu}!}{N}\left[1 + O(\Delta)\right], \quad \boldsymbol{\mu}! \equiv \mu_X! \mu_Y!. \tag{2.17}$$

The CRB is valid for any estimator $\check{\theta}_{\boldsymbol{\mu}}$ that satisfies the unbiased condition

$$\mathbb{E}\left(\check{\theta}_{\boldsymbol{\mu}}\right) = \theta_{\boldsymbol{\mu}}. \tag{2.18}$$

A Bayesian version of the CRB valid for any biased or unbiased estimator is available [5, 24] but not considered here, as it would offer qualitatively similar conclusions for the present problem.

III. MOMENT ESTIMATION BY SPADE

A. TEM scheme

Consider the transverse-electromagnetic (TEM) basis given by $\{\phi_{\boldsymbol{q}}(\boldsymbol{r}); \boldsymbol{q} = (q_x, q_y) \in \mathbb{N}^2\}$, where

$$\phi_{\boldsymbol{q}}(\boldsymbol{r}) = \frac{\mathrm{He}_{q_x}(x)\,\mathrm{He}_{q_y}(y)}{\sqrt{2\pi \boldsymbol{q}!}} e^{-|\boldsymbol{r}|^2/4}, \tag{3.1}$$

and He_q is a Hermite polynomial [25, 26]. Using the generating function $\exp(xz - z^2/2) = \sum_{q=0}^{\infty} \mathrm{He}_q(x) z^q/q!$ [25, 26], it can be shown that

$$\psi(\boldsymbol{r} - \boldsymbol{R}) = e^{-|\boldsymbol{R}|^2/8} \sum_{\boldsymbol{q} \in \mathbb{N}^2} \frac{\boldsymbol{R}^{\boldsymbol{q}}}{2^{|\boldsymbol{q}|_1}\sqrt{\boldsymbol{q}!}} \phi_{\boldsymbol{q}}(\boldsymbol{r}), \tag{3.2}$$

$$|\boldsymbol{q}|_1 \equiv q_x + q_y. \tag{3.3}$$

The expected photon count given by Eq. (2.6) in a TEM mode becomes [13, 16]

$$\bar{m}_{\boldsymbol{q}} = N^{(\mathrm{TEM})} C(\boldsymbol{q}, \boldsymbol{q}) \Theta_{2\boldsymbol{q}}, \tag{3.4}$$

$$C(\boldsymbol{q}, \boldsymbol{q}') \equiv \frac{1}{2^{|\boldsymbol{q}+\boldsymbol{q}'|_1}\sqrt{\boldsymbol{q}!\boldsymbol{q}'!}}, \tag{3.5}$$

$$\Theta_{\boldsymbol{\mu}} \equiv \int d^2\boldsymbol{R} \boldsymbol{R}^{\boldsymbol{\mu}} e^{-|\boldsymbol{R}|^2/4} F(\boldsymbol{R}|\theta), \tag{3.6}$$

where the superscript in $N^{(\mathrm{TEM})}$ emphasizes that the TEM scheme may take only a fraction of the available photons in practice.

To proceed, Ref. [16] simply assumes $\Theta_{\boldsymbol{\mu}} \approx \theta_{\boldsymbol{\mu}}$ for subdiffraction objects, without quantifying the systematic errors that may arise from such an approximation. Here I consider the exact relation given by

$$\theta_{\boldsymbol{\mu}} = \int d^2\boldsymbol{R} \boldsymbol{R}^{\boldsymbol{\mu}} e^{|\boldsymbol{R}|^2/4} e^{-|\boldsymbol{R}|^2/4} F(\boldsymbol{R}|\theta) \tag{3.7}$$

$$= \int d^2\boldsymbol{R} \boldsymbol{R}^{\boldsymbol{\mu}} \left[\sum_{\boldsymbol{p} \in \mathbb{N}^2} C(\boldsymbol{p}, \boldsymbol{p}) \boldsymbol{R}^{2\boldsymbol{p}}\right] e^{-|\boldsymbol{R}|^2/4} F(\boldsymbol{R}|\theta) \tag{3.8}$$

$$= \sum_{\boldsymbol{p} \in \mathbb{N}^2} C(\boldsymbol{p}, \boldsymbol{p}) \Theta_{\boldsymbol{\mu}+2\boldsymbol{p}}. \tag{3.9}$$

This linear relation implies that an unbiased estimator of $\theta_{\boldsymbol{\mu}}$ can be constructed from unbiased estimators of $\Theta_{\boldsymbol{\mu}+2\boldsymbol{p}}$ as

$$\check{\theta}_{\boldsymbol{\mu}} = \sum_{\boldsymbol{p} \in \mathbb{N}^2} C(\boldsymbol{p}, \boldsymbol{p}) \check{\Theta}_{\boldsymbol{\mu}+2\boldsymbol{p}}. \tag{3.10}$$

For example, given the photon counts $\{m_{\boldsymbol{q}}\}$ from the TEM scheme, an unbiased estimator of the moment $\theta_{2\boldsymbol{q}}$ is

$$\check{\theta}_{2\boldsymbol{q}} = \sum_{\boldsymbol{p} \in \mathbb{N}^2} C(\boldsymbol{p}, \boldsymbol{p}) \check{\Theta}_{2\boldsymbol{q}+2\boldsymbol{p}}, \tag{3.11}$$

$$\check{\Theta}_{2\boldsymbol{q}+2\boldsymbol{p}} = \frac{m_{\boldsymbol{q}+\boldsymbol{p}}}{N^{(\mathrm{TEM})} C(\boldsymbol{q}+\boldsymbol{p}, \boldsymbol{q}+\boldsymbol{p})}. \tag{3.12}$$

The unbiased conditions

$$\mathbb{E}(\check{\Theta}_{2\boldsymbol{q}+2\boldsymbol{p}}) = \Theta_{2\boldsymbol{q}+2\boldsymbol{p}}, \qquad \mathbb{E}(\check{\theta}_{2\boldsymbol{q}}) = \theta_{2\boldsymbol{q}} \tag{3.13}$$

can be derived from Eqs. (3.4) and (3.9). The mean-square error, on the other hand, is

$$\mathbb{E}\left(\check{\theta}_{2\boldsymbol{q}} - \theta_{2\boldsymbol{q}}\right)^2 = \mathbb{V}\left(\check{\theta}_{2\boldsymbol{q}}\right) \tag{3.14}$$

$$= \sum_{\boldsymbol{p}\in\mathbb{N}^2} C^2(\boldsymbol{p},\boldsymbol{p})\mathbb{V}\left(\check{\Theta}_{2\boldsymbol{q}+2\boldsymbol{p}}\right), \tag{3.15}$$

$$\mathbb{V}\left(\check{\Theta}_{2\boldsymbol{q}+2\boldsymbol{p}}\right) = \frac{\Theta_{2\boldsymbol{q}+2\boldsymbol{p}}}{N^{(\mathrm{TEM})}C(\boldsymbol{q}+\boldsymbol{p},\boldsymbol{q}+\boldsymbol{p})}, \tag{3.16}$$

where

$$\mathbb{V}\left(f\right) \equiv \mathbb{E}\left(f^2\right) - \mathbb{E}^2\left(f\right) \tag{3.17}$$

is the variance. With

$$|\Theta_{\boldsymbol{\mu}}| \le \left(\frac{\Delta}{2}\right)^{|\boldsymbol{\mu}|_1}, \tag{3.18}$$

the convergence of Eq. (3.15) can be proved using the ratio test [27]. Equation (3.18) also means that, in the subdiffraction regime, Eq. (3.15) is dominated by the leading-order term

$$\mathbb{V}(\check{\Theta}_{2\boldsymbol{q}}) = \frac{\Theta_{2\boldsymbol{q}}}{N^{(\mathrm{TEM})}C(\boldsymbol{q},\boldsymbol{q})} \le \frac{\boldsymbol{q}!\Delta^{2|\boldsymbol{q}|_1}}{N^{(\mathrm{TEM})}}. \tag{3.19}$$

Compared with the CRB for direct imaging given by Eq. (2.17), the error of the TEM scheme for each moment can be significantly smaller when $\Delta \ll 1$. The enhancement can be attributed to the coherent filtering of the low-order modes, which act as background noise to direct imaging, and the low variances of the darker high-order outputs.

In practice, only a finite number of channels can be measured. Consider the finite-channel estimator

$$\check{\theta}'_{2\boldsymbol{q}} = \sum_{\boldsymbol{p}=(0,0)}^{\boldsymbol{p}'} C(\boldsymbol{p},\boldsymbol{p})\check{\Theta}_{2\boldsymbol{q}+2\boldsymbol{p}}, \tag{3.20}$$

which uses only modes with orders from $\boldsymbol{q}$ to $\boldsymbol{q}+\boldsymbol{p}'$ and now has a bias given by

$$\mathbb{E}\left(\check{\theta}'_{2\boldsymbol{q}}\right) - \theta_{2\boldsymbol{q}} = O\left(\Delta^{2|\boldsymbol{q}|_1+2|\boldsymbol{p}'|_1+2}\right). \tag{3.21}$$

The estimation error becomes

$$\mathbb{E}\left(\check{\theta}'_{2\boldsymbol{q}} - \theta_{2\boldsymbol{q}}\right)^2 = \mathbb{V}\left(\check{\theta}'_{2\boldsymbol{q}}\right) + \left[\mathbb{E}\left(\check{\theta}'_{2\boldsymbol{q}}\right) - \theta_{2\boldsymbol{q}}\right]^2 \tag{3.22}$$

$$= \frac{O(\Delta^{2|\boldsymbol{q}|_1})}{N^{(\mathrm{TEM})}} + O\left(\Delta^{4|\boldsymbol{q}|_1+4|\boldsymbol{p}'|_1+4}\right). \tag{3.23}$$

Unlike the estimator variance, the error due to the bias does not scale with the photon number. The measured modes should therefore be chosen such that the total error remains acceptable. For example, the numerical demonstration in Ref. [16] assumes simply $\check{\theta}'_{2\boldsymbol{q}} = \check{\Theta}_{2\boldsymbol{q}}$ but still obtains satisfactory results.

B. iTEM1 and iTEM4 schemes

The interferometric TEM (iTEM) measurement proposed in Ref. [16] assumes the following pair of projections:

$$\phi_+^{(\boldsymbol{q},\boldsymbol{q}')}(\boldsymbol{r}) = \frac{1}{\sqrt{2}}\left[\phi_{\boldsymbol{q}}(\boldsymbol{r}) + \phi_{\boldsymbol{q}'}(\boldsymbol{r})\right], \tag{3.24}$$

$$\phi_-^{(\boldsymbol{q},\boldsymbol{q}')}(\boldsymbol{r}) = \frac{1}{\sqrt{2}}\left[\phi_{\boldsymbol{q}}(\boldsymbol{r}) - \phi_{\boldsymbol{q}'}(\boldsymbol{r})\right]. \tag{3.25}$$

The expected photon counts are

$$\bar{m}_+^{(\boldsymbol{q},\boldsymbol{q}')} = N\left[\beta(\boldsymbol{q},\boldsymbol{q}') + C(\boldsymbol{q},\boldsymbol{q}')\Theta_{\boldsymbol{q}+\boldsymbol{q}'}\right], \tag{3.26}$$

$$\bar{m}_-^{(\boldsymbol{q},\boldsymbol{q}')} = N\left[\beta(\boldsymbol{q},\boldsymbol{q}') - C(\boldsymbol{q},\boldsymbol{q}')\Theta_{\boldsymbol{q}+\boldsymbol{q}'}\right], \tag{3.27}$$

$$\beta(\boldsymbol{q},\boldsymbol{q}') \equiv \frac{1}{2}\left[C(\boldsymbol{q},\boldsymbol{q})\Theta_{2\boldsymbol{q}} + C(\boldsymbol{q}',\boldsymbol{q}')\Theta_{2\boldsymbol{q}'}\right]. \tag{3.28}$$

Given the two photon counts $m_+^{(\boldsymbol{q},\boldsymbol{q}')}$ and $m_+^{(\boldsymbol{q},\boldsymbol{q}')}$, an unbiased estimator of $\Theta_{\boldsymbol{q}+\boldsymbol{q}'}$ can be constructed as

$$\check{\Theta}_{\boldsymbol{q}+\boldsymbol{q}'} = \frac{m_+^{(\boldsymbol{q},\boldsymbol{q}')} - m_-^{(\boldsymbol{q},\boldsymbol{q}')}}{2NC(\boldsymbol{q},\boldsymbol{q}')}, \tag{3.29}$$

$$\mathbb{V}\left(\check{\Theta}_{\boldsymbol{q}+\boldsymbol{q}'}\right) = \frac{\beta(\boldsymbol{q},\boldsymbol{q}')}{2NC^2(\boldsymbol{q},\boldsymbol{q}')} \tag{3.30}$$

$$= \frac{O(\Delta^{2\min(|\boldsymbol{q}|_1,|\boldsymbol{q}'|_1)})}{N}. \tag{3.31}$$

Multiple iTEM measurements can be applied simultaneously as long as the projections are orthogonal; Fig. 1 depicts the 7 sets of orthogonal projections proposed in Ref. [16] for the estimation of all $\Theta_{\boldsymbol{\mu}}$.

The iTEM1 scheme consists of projections with

$$q_x \in \{0,2,4,\dots\}, \qquad q_y \in \{0,1,2,\dots\}, \tag{3.32}$$

$$\boldsymbol{q}' = \boldsymbol{q} + (1,0), \tag{3.33}$$

such that it is sensitive to $\Theta_{\boldsymbol{\mu}}$ with

$$\mu_X \in \{1,5,9,\dots\}, \qquad \mu_Y \in \{0,2,4,\dots\}, \tag{3.34}$$

while the iTEM4 scheme consists of projections with

$$q_x \in \{1,3,5,\dots\}, \qquad q_y \in \{0,1,2,\dots\}, \tag{3.35}$$

$$\boldsymbol{q}' = \boldsymbol{q} + (1,0), \tag{3.36}$$

such that it is sensitive to $\Theta_{\boldsymbol{\mu}}$ with

$$\mu_X \in \{3,7,11,\dots\}, \qquad \mu_Y \in \{0,2,4,\dots\}. \tag{3.37}$$

The two schemes together offer sensitivity to any $\Theta_{\boldsymbol{\mu}}$ with odd μ_X and even μ_Y, allowing an unbiased estimator of $\theta_{\boldsymbol{\mu}}$ with odd μ_X and even μ_Y to be constructed from their outputs according to Eqs. (3.10) and (3.29). Assuming that the iTEM1 scheme receives $N^{(\mathrm{iTEM1})}$ photons on average and the iTEM4 scheme also receives $O(N^{(\mathrm{iTEM1})})$ photons, Eq. (3.31) leads to

$$\mathbb{V}(\check{\Theta}_{\boldsymbol{\mu}}) = \frac{O\left(\Delta^{|\boldsymbol{\mu}|_1-1}\right)}{N^{(\mathrm{iTEM1})}}, \tag{3.38}$$

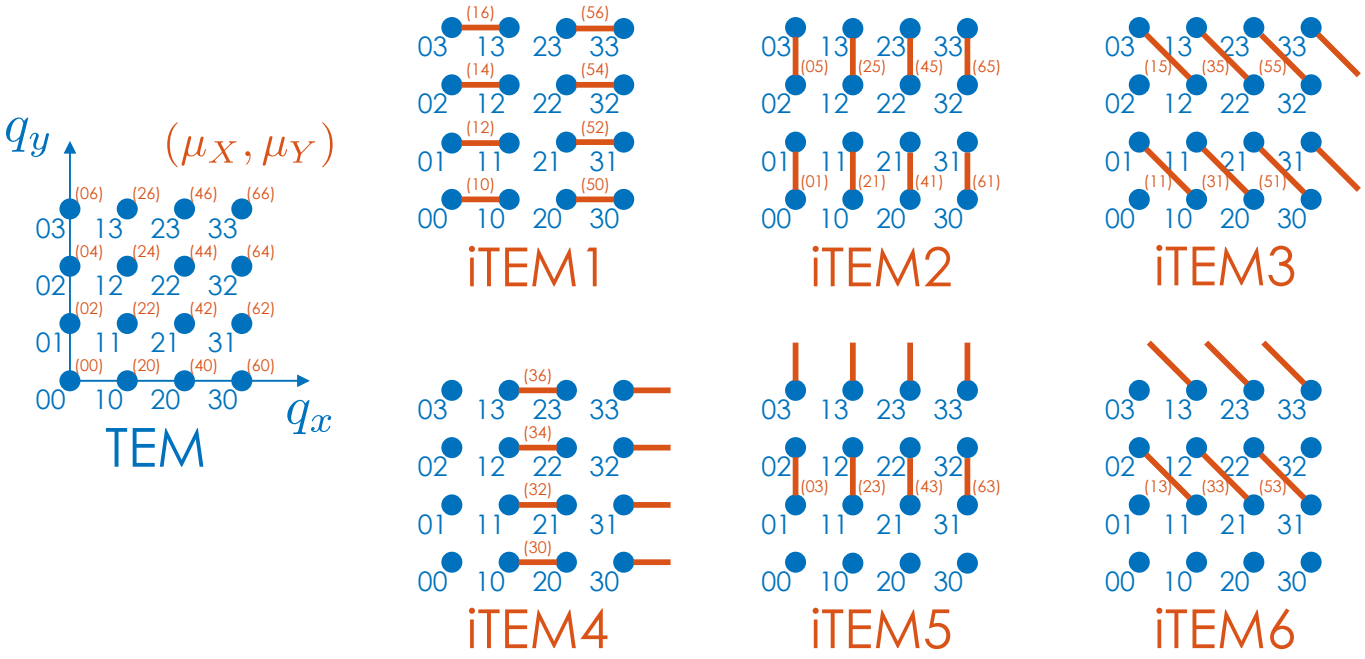

FIG. 1. Each dot corresponds to a TEM mode with mode function $\phi_{\boldsymbol{q}}(\boldsymbol{r})$ in the (q_x, q_y) space, and each line connecting two dots denotes an interferometer between two TEM modes, resulting in the mode functions $[\phi_{\boldsymbol{q}}(\boldsymbol{r}) \pm \phi_{\boldsymbol{q}'}(\boldsymbol{r})]/\sqrt{2}$ in an iTEM scheme. Each bracketed number is the order (μ_X, μ_Y) of the object parameter $\Theta_{\boldsymbol{\mu}}$ to which a projection is sensitive.

and the error becomes

$$\mathbb{E}\left(\check{\theta}_{\boldsymbol{\mu}} - \theta_{\boldsymbol{\mu}}\right)^2 = \mathbb{V}\left(\check{\theta}_{\boldsymbol{\mu}}\right) \tag{3.39}$$

$$= \sum_{\boldsymbol{p}\in\mathbb{N}^2} C^2(\boldsymbol{p},\boldsymbol{p})\mathbb{V}\left(\check{\Theta}_{\boldsymbol{\mu}+2\boldsymbol{p}}\right) \tag{3.40}$$

$$= \frac{O(\Delta^{|\boldsymbol{\mu}|_1-1})}{N^{(\mathrm{iTEM1})}}, \tag{3.41}$$

which can offer substantial improvements over the direct-imaging CRB given by Eq. (2.17) for the $|\boldsymbol{\mu}|_1 > 1$ moments.

With a finite number of channels, the estimator

$$\check{\theta}'_{\boldsymbol{\mu}} = \sum_{\boldsymbol{p}=(0,0)}^{\boldsymbol{p}'} C(\boldsymbol{p},\boldsymbol{p})\check{\Theta}_{\boldsymbol{\mu}+2\boldsymbol{p}} \tag{3.42}$$

has a bias

$$\mathbb{E}\left(\check{\theta}'_{\boldsymbol{\mu}}\right) - \theta_{\boldsymbol{\mu}} = O\left(\Delta^{|\boldsymbol{\mu}|_1+2|\boldsymbol{p}'|_1+2}\right), \tag{3.43}$$

and the error becomes

$$\mathbb{E}\left(\check{\theta}'_{\boldsymbol{\mu}} - \theta_{\boldsymbol{\mu}}\right)^2 = \frac{O(\Delta^{|\boldsymbol{\mu}|_1-1})}{N^{(\mathrm{iTEM1})}} + O\left(\Delta^{2|\boldsymbol{\mu}|_1+4|\boldsymbol{p}'|_1+4}\right). \tag{3.44}$$

$\boldsymbol{p}'$ should again be chosen to keep the total error acceptable in practice.

C. iTEM2 and iTEM5 schemes

The analysis of the iTEM2 and iTEM5 schemes is identical to that in Sec. III B, except that the x and y dimensions are switched. The iTEM2 scheme consists of projections with

$$q_x \in \{0,1,2,\dots\}, \qquad q_y \in \{0,2,4,\dots\}, \tag{3.45}$$

$$\boldsymbol{q}' = \boldsymbol{q} + (0,1), \tag{3.46}$$

such that it is sensitive to $\Theta_{\boldsymbol{\mu}}$ with

$$\mu_X \in \{0,2,4,\dots\}, \qquad \mu_Y \in \{1,5,9,\dots\}, \tag{3.47}$$

while the iTEM5 scheme consists of projections with

$$q_x \in \{0,1,2,\dots\}, \qquad q_y \in \{1,3,5,\dots\}, \tag{3.48}$$

$$\boldsymbol{q}' = \boldsymbol{q} + (0,1), \tag{3.49}$$

such that it is sensitive to $\Theta_{\boldsymbol{\mu}}$ with

$$\mu_X \in \{0,2,4,\dots\}, \qquad \mu_Y \in \{3,7,11,\dots\}. \tag{3.50}$$

An unbiased estimator of $\theta_{\boldsymbol{\mu}}$ with even μ_X and odd μ_Y can be constructed from the outputs of the two schemes according to Eqs. (3.10) and (3.29). Assuming that the iTEM2 scheme receives $N^{(\mathrm{iTEM2})}$ photons and the iTEM5 scheme also receives $O(N^{(\mathrm{iTEM2})})$ photons, the estimation errors have the same expressions as Eqs. (3.41) and (3.44), with $N^{(\mathrm{iTEM2})}$ replacing $N^{(\mathrm{iTEM1})}$.

D. iTEM3 and iTEM6 schemes

The iTEM3 scheme consists of projections with

$$q_x \in \{0,1,2,\dots\}, \qquad q_y \in \{1,3,5,\dots\}, \tag{3.51}$$

$$\boldsymbol{q}' = \boldsymbol{q} + (1,-1), \tag{3.52}$$

such that it is sensitive to $\Theta_{\boldsymbol{\mu}}$ with

$$\mu_X \in \{1,3,5,\dots\}, \qquad \mu_Y \in \{1,5,9,\dots\}, \tag{3.53}$$

while the iTEM6 scheme consists of projections with

$$q_x \in \{0,1,2,\dots\}, \qquad q_y \in \{2,4,6,\dots\}, \tag{3.54}$$
$$\boldsymbol{q}' = \boldsymbol{q} + (1,-1), \tag{3.55}$$

such that it is sensitive to $\Theta_{\boldsymbol{\mu}}$ with

$$\mu_X \in \{1,3,5,\dots\}, \qquad \mu_Y \in \{3,7,11,\dots\}. \tag{3.56}$$

An unbiased estimator of $\theta_{\boldsymbol{\mu}}$ with odd μ_X and odd μ_Y can be constructed from the outputs of the iTEM3 and iTEM6 schemes according to Eqs. (3.10) and (3.29). Assuming that the iTEM3 scheme receives $N^{(\text{iTEM3})}$ photons on average and the iTEM6 scheme also receives $O(N^{(\text{iTEM3})})$ photons, Eq. (3.31) implies

$$\mathbb{V}\left(\check{\Theta}_{\boldsymbol{\mu}}\right) = \frac{O(\Delta^{|\boldsymbol{\mu}|_1})}{N^{(\text{iTEM3})}}. \tag{3.57}$$

The error becomes

$$\mathbb{E}\left(\check{\theta}_{\boldsymbol{\mu}} - \theta_{\boldsymbol{\mu}}\right)^2 = \frac{O(\Delta^{|\boldsymbol{\mu}|_1})}{N^{(\text{iTEM3})}} \tag{3.58}$$

for the estimator given by Eq. (3.10), and

$$\mathbb{E}\left(\check{\theta}'_{\boldsymbol{\mu}} - \theta_{\boldsymbol{\mu}}\right)^2 = \frac{O(\Delta^{|\boldsymbol{\mu}|_1})}{N^{(\text{iTEM3})}} + O\left(\Delta^{2|\boldsymbol{\mu}|_1+4|\boldsymbol{p}'|_1+4}\right) \tag{3.59}$$

for the finite-channel estimator given by Eq. (3.42).

IV. DISCUSSION

The semiclassical treatment here complements the quantum approach in Ref. [16] by offering a shortcut to the Poisson photon-counting model for weak incoherent sources, passive linear optics, and photon counting. Besides pedagogy, this work presents a new form of estimators and more rigorous expressions for their errors, without resorting to the $\Theta_{\boldsymbol{\mu}} \approx \theta_{\boldsymbol{\mu}}$ approximation used in Ref. [16] or asymptotic arguments. The resulting errors turn out to be on the same orders as the ones suggested in Ref. [16]. The conclusion of Ref. [16] hence remains intact: compared with direct imaging, SPADE can estimate the second and higher moments of subdiffraction objects much more precisely.

The linear form of the estimators is chosen here on account of its tractability, but nonlinear estimators may perform even better. For example, the maximum-likelihood estimator [24] for this problem can combine all the outputs of the different schemes and would be nonlinear, while more advanced estimators in modern Bayesian or minimax statistics may also help.

Experimental implementations and generalizations for non-Gaussian point-spread functions are important future directions. For proof-of-concept demonstrations, it should be possible to use the same setups described in Refs. [12–15] to estimate at least the second moments of more general objects. For other point-spread functions, the theory outlined in Refs. [9, 11] seems promising.

To bring SPADE into practice for fluorescence microscopy and telescopy, efficient demultiplexing for broadband sources is needed. The technical challenges are by no means trivial, but the promise of giant enhancements using only far-field linear optics should motivate further efforts.

ACKNOWLEDGMENTS

This work is supported by the Singapore Ministry of Education Academic Research Fund Tier 1 Project R-263-000-C06-112.

[1] M. Tsang, R. Nair, and X.-M. Lu, Physical Review X **6**, 031033 (2016).
[2] R. Nair and M. Tsang, Optics Express **24**, 3684 (2016).
[3] M. Tsang, R. Nair, and X.-M. Lu, in *Proc. SPIE*, Quantum and Nonlinear Optics IV, Vol. 10029 (2016) p. 1002903.
[4] R. Nair and M. Tsang, Physical Review Letters **117**, 190801 (2016).
[5] M. Tsang, arXiv:1605.03799 [physics, physics:quant-ph] (2017).
[6] S. Z. Ang, R. Nair, and M. Tsang, arXiv:1606.00603 [physics, physics:quant-ph] (2016).
[7] X.-M. Lu, R. Nair, and M. Tsang, arXiv:1609.03025 [quant-ph] (2016).
[8] C. Lupo and S. Pirandola, Physical Review Letters **117**, 190802 (2016).
[9] J. Rehacek, M. Paúr, B. Stoklasa, Z. Hradil, and L. L. Sánchez-Soto, Optics Letters **42**, 231 (2017).
[10] H. Krovi, S. Guha, and J. H. Shapiro, arXiv:1609.00684 [physics, physics:quant-ph] (2016).
[11] R. Kerviche, S. Guha, and A. Ashok, arXiv:1701.04913 [physics, physics:quant-ph] (2017).
[12] Z. S. Tang, K. Durak, and A. Ling, Optics Express **24**, 22004 (2016).
[13] F. Yang, A. Tashchilina, E. S. Moiseev, C. Simon, and A. I. Lvovsky, Optica **3**, 1148 (2016).
[14] W.-K. Tham, H. Ferretti, and A. M. Steinberg, Physical Review Letters **118**, 070801 (2017).
[15] M. Paúr, B. Stoklasa, Z. Hradil, L. L. Sánchez-Soto, and J. Rehacek, Optica **3**, 1144 (2016).
[16] M. Tsang, New Journal of Physics **19**, 023054 (2017).
[17] J. W. Goodman, *Introduction to Fourier Optics* (McGraw-Hill, New York, 2004).
[18] J. W. Goodman, *Statistical Optics* (Wiley, New York, 1985).
[19] D. A. B. Miller, Optics Express **20**, 23985 (2012).

[20] J. Zmuidzinas, J. Opt. Soc. Am. A **20**, 218 (2003).
[21] M. C. E. Huber, A. Pauluhn, J. L. Culhane, J. G. Timothy, K. Wilhelm, and A. Zehnder, eds., *Observing Photons in Space: A Guide to Experimental Space Astronomy* (Springer, New York, 2013).
[22] H. Deschout, F. C. Zanacchi, M. Mlodzianoski, A. Diaspro, J. Bewersdorf, S. T. Hess, and K. Braeckmans, Nature Methods **11**, 253 (2014).
[23] J. Chao, E. Sally Ward, and R. J. Ober, Journal of the Optical Society of America A **33**, B36 (2016).
[24] H. L. Van Trees, *Detection, Estimation, and Modulation Theory, Part I.* (John Wiley & Sons, New York, 2001).
[25] DLMF, "NIST Digital Library of Mathematical Functions," http://dlmf.nist.gov/, Release 1.0.11 of 2016-06-08 (2016), online companion to [26].
[26] F. W. J. Olver, D. W. Lozier, R. F. Boisvert, and C. W. Clark, eds., *NIST Handbook of Mathematical Functions* (Cambridge University Press, New York, NY, 2010) print companion to [25].
[27] G. B. Arfken and H. J. Weber, *Mathematical Methods for Physicists* (Elsevier, Amsterdam, 2005).